SURFACE SCIENCE 13 (1969) 72–84 © North-Holland Publishing Co., Amsterdam

POLAR SURFACES OF ZINC OXIDE CRYSTALS

G. HEILAND and P. KUNSTMANN

2. Physikalisches Institut, Rheinisch-Westfälische Technische Hochschule, Aachen, Germany

Received 30 April 1968

Polar surfaces have been prepared by cleavage in ultrahigh vacuum. The electrical conductivity at these surfaces has been studied between 90 and 600 °K. Changes occur by annealing in vacuum and by adsorption of atomic hydrogen or of oxygen. Additional information is obtained from cleaving crystals under mercury and measuring the current versus voltage relation. Furthermore, changes of the reflectance of light have been observed which are induced by adsorption of atomic hydrogen or of oxygen.

For clean polar surfaces the conductivity must be below an upper limit of 4×10^{-12} A/V. Transient heating in vacuum produces a high surface conductivity of 10^{-4} A/V on the Zn surface whereas the O surface does not change. Atomic hydrogen acts much faster on the O surface than on the Zn surface creating an accumulation layer of high conductivity. By contrast, the depletion layer caused by the adsorption of oxygen is more evident on the Zn surface. The results of the optical measurements support these data.

An atomic model of the polar surfaces is discussed. Several arguments concerning the distribution of electrons at these surfaces are considered in connection with the idea of dangling bonds and with compensation of the internal dipole moment of the wurtzite structure.

1. Introduction

The hexagonal wurtzite structure of ZnO is noncentrosymmetric and exhibits a polar c axis (fig. 1). Therefore not only piezoelectric but also pyroelectric effects have been observed[1]). The structure can be described as a series of atomic double layers which are normal to the c axis. The series terminates with the two polar $\{0001\}$ surfaces, which are different with regard to the direction of the c axis. They are designated as Zn surface and O surface. There is no proof that the double layers are not split at the surface, but the arrangement of bonds provides an argument: Within these double layers the atoms are triply bonded whereas only a single bond per atom exists between the double layers.

After calibration by X-ray diffraction the sign of the c axis can easily be determined merely by etching the polar surfaces[2,3]). Similar studies have been performed for other binary compounds with zinc-blende or wurtzite structure[4–6,18]). Fig. 2 shows a twin crystal with the c axes antiparallel. Etch pits on $\{10\bar{1}0\}$ prism faces of the hexagonal needles ($\| c$) also allow a

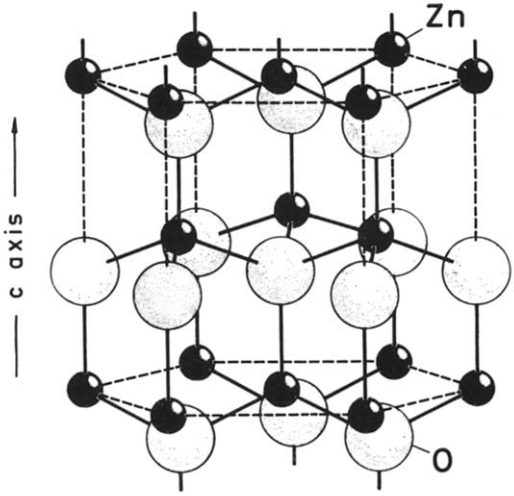

Fig. 1. Wurtzite structure of ZnO.

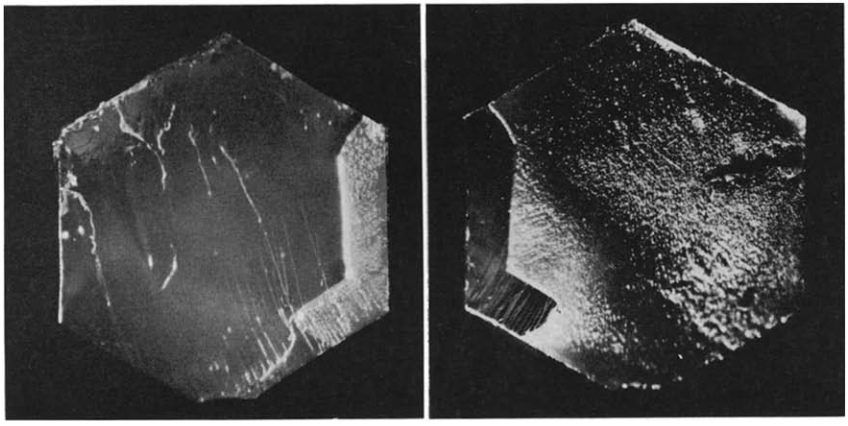

(a) (b)

Fig. 2. Cleaved and etched surfaces of a twin crystal (HCl, 6%). (a) The greater part exhibits the etching behavior of a Zn surface, the smaller of an O surface, c axes antiparallel. (b) The other cleavage face shows the reverse behavior. 37 ×. After Heiland et al.[3]).

determination of the polar axis (fig. 3). In an ideal and clean state these prism faces expose Zn and O atoms in equal numbers.

The electrical properties of the prism surfaces were studied several years ago[8-10]), but up to now nothing is known about those of the polar surfaces.

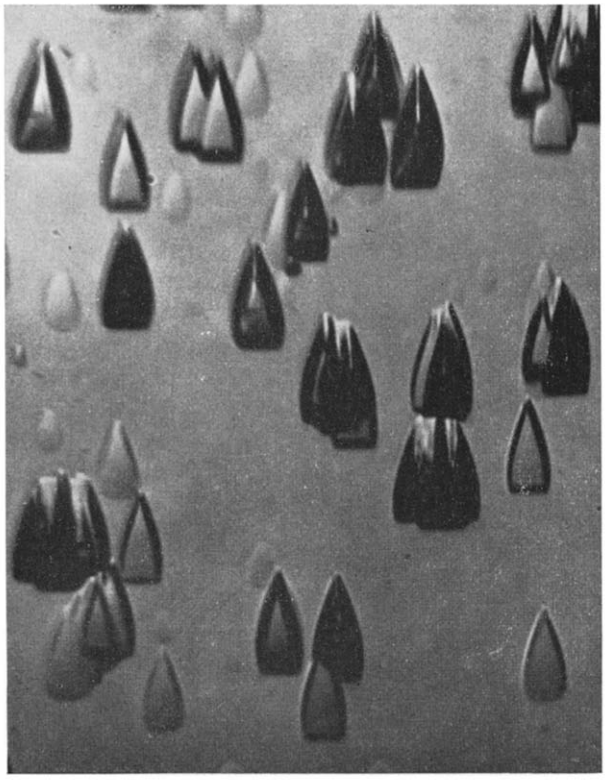

Fig. 3. Prism face etched in HF, 40%. The etch pits point in the positive direction of the c axis. 100 $\times$. After Klein[7]).

Therefore a series of experiments was undertaken to observe and compare electrical and optical properties of the Zn and O surfaces.

2. Space-charge layers and surface conductivity

Some electrical properties of the prism faces, e.g., surface conductivity, field effect and surface photoconductivity can be changed through several orders of magnitude by a prior treatment of the crystal with oxygen or atomic hydrogen at room temperature. This has been related to the term structure of electronic surface states[10]). The adsorbed oxygen binds electrons from the crystal (always n-type) and creates a depletion layer of low conductivity, whereas atomic hydrogen produces surface donors and an accumulation layer of high conductivity (fig. 4).

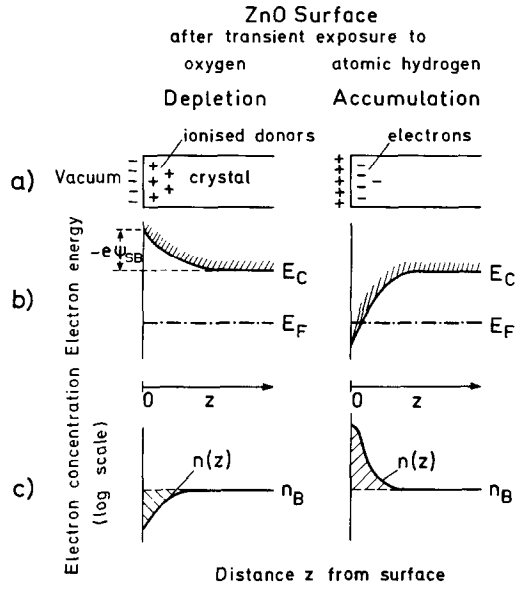

Fig. 4. Space charge layers on the surface of ZnO. (a) Distribution of charges, (b) band scheme, (c) electron concentration.

A sheet conductance can be defined as:

$$g_{\square} = e\int_0^l \mu n \, dz =$$

$$= e\int_0^l \mu_B n_B \, dz + e\int_0^d \mu_B [n(z) - n_B] \, dz - e\int_0^d (\mu_B - \mu_S) \, n(z) \, dz =$$

$$= \sigma_B l + \Delta\sigma,$$

where

μ_B = bulk mobility of electrons,
μ_S = surface mobility of electrons,
n_B = bulk concentration of electrons,
σ_B = bulk conductivity,
$\Delta\sigma$ = surface conductivity,
l = thickness of the sheet,
d = thickness of the space-charge layer, $d<l$,
z = space coordinate normal to the surface,
$\Delta N = \int_0^l [n(z) - n_B] \, dz$ = excess of electrons in the space charge layer (fig. 4, shaded region).

The last of the three terms in $g_\square$ can be neglected if $\mu_S = \mu_B$. Only for surface conductivities above 10^{-5} A/V does the calculated surface mobility of zinc oxide drop below the bulk value[11]). In the present work it often holds that

$$\sigma_B l \ll \Delta\sigma = e\mu_S \Delta N .$$

The surface conductivity can be computed as a function of band bending and is shown schematically in fig. 5.

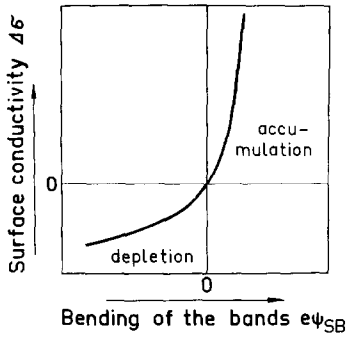

Fig. 5. Schematic representation of surface conductivity versus bending of the bands (cf. fig. 4).

3. Experimental

The ZnO crystals were grown from the vapor phase in the form of hexagonal prisms having a diameter of 1–3 mm and a length of 30–40 mm. An addition of copper lowered the bulk conductivity to 10^{-4}–10^{-5} ohm^{-1} cm^{-1}. Fig. 6 shows a crystal with gold contacts for measurement of the sheet conductance by the method of van der Pauw[17]). Stabilization against heating in vacuum and influences of gases was achieved by deposition of a pyrolytic quartz film which covered also the contacts (fig. 6). Subsequent cleavage in

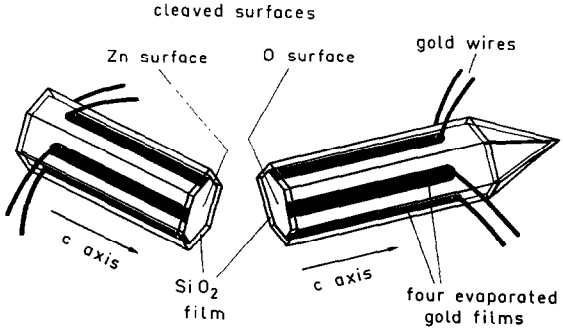

Fig. 6. ZnO crystal after preparation and cleavage[11]).

ultrahigh vacuum exposed only the polar surfaces. By control experiments it was confirmed that all observed surface effects took place on the polar surfaces. After baking the vacuum was below 10^{-9} Torr.

Before cleavage under Hg the crystals were covered with resin. For the reflectance measurements the crystals were cleaved in air, subsequently annealed and measured in a vacuum of 10^{-7} Torr.

4. Results

4.1. Surface conductivity of clean surfaces

After cleavage at 90°K no surface conductivity was deptected ($\Delta\sigma < 4 \times 10^{-12}$ A/V). But a transient warming up to about 300°C in vacuum resulted in a marked change on the Zn surfaces (fig. 7). The steep curve

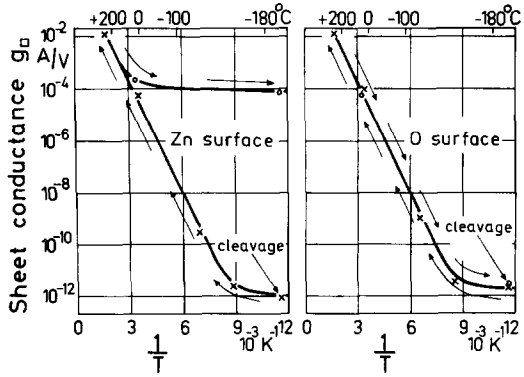

Fig. 7. Sheet conductance versus temperature after cleavage in vacuum[11]).

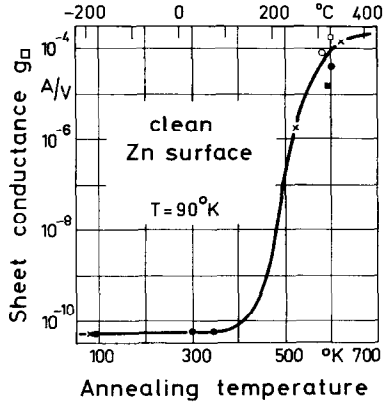

Fig. 8. Annealing curve for six different crystals (ref. 11) (cf. fig. 7).

represents the contribution of the bulk. The O surface follows the same curve upon cooling down after heating, but the Zn surface retains a high surface conductivity which is independent of temperature and can be removed by transient admission of oxygen at room temperature. Reheating produces the same high surface conductivity of 10^{-4} A/V (100 μmhos). The result of annealing is shown in fig. 8.

4.2. Change of surface conductivity by hydrogen and oxygen

No surface conductivity was created by molecular hydrogen (0.1–10 Torr) at room temperature, but as soon as the molecules were dissociated by a tungsten filament, the surface conductivity rose. Fig. 9 shows that for a given exposure time the increase on the O-surface exceeded that on the Zn surface by one or two orders of magnitude. In all cases the final saturation values nearly coincided. A subsequent transient treatment with oxygen at room temperature resulted again in a different change of surface conductivity. This time the Zn surface reacted faster, as evidenced by the decrease of conductivity (fig. 10). After sufficient time in oxygen (20–60 min) the conductivity subsided on both surfaces.

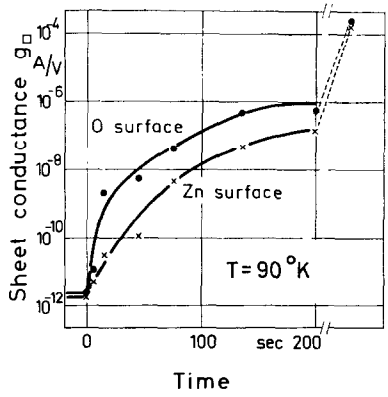

Fig. 9. Surface conductivity generated by atomic hydrogen[11]).

The action of oxygen in binding conduction electrons can be detected by a decrease of sheet conductance only if there is a measurable surface conductivity. Thus it was impossible to study freshly cleaved surfaces. For the investigation of depletion layers, it is essential to measure the conductance normal, rather than parallel to the surface. To this end crystals were cleaved under mercury[12]). Fig. 11 shows that initially there is no rectification, i.e. no depletion on the Zn surface. The same holds for the O surface. Perhaps

after some time oxygen reaches the surfaces through the metal. After deliberate exposure to air (oxygen) the depletion layer is more pronounced on the Zn surface. This corresponds to results with gold films evaporated on oxygen covered polar surfaces. Again the Zn surfaces show the stronger depletion layer[12]).

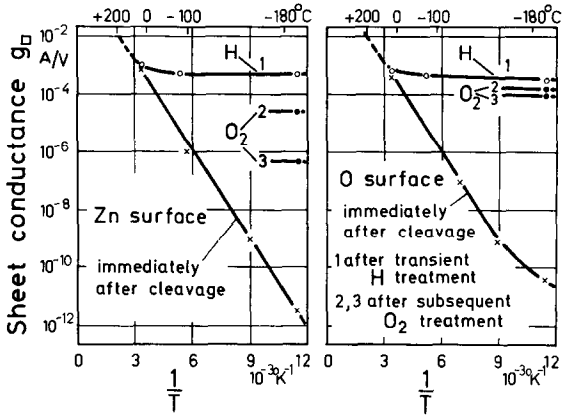

Fig. 10. Sheet conductance measured in vacuum versus temperature. After a pretreatment with atomic hydrogen (curve 1), oxygen was admitted. (curve 2) 3×10^{-3} Torr O_2, 10 min; (curve 3) 10^{-2} Torr O_2, 10 min (ref. 11).

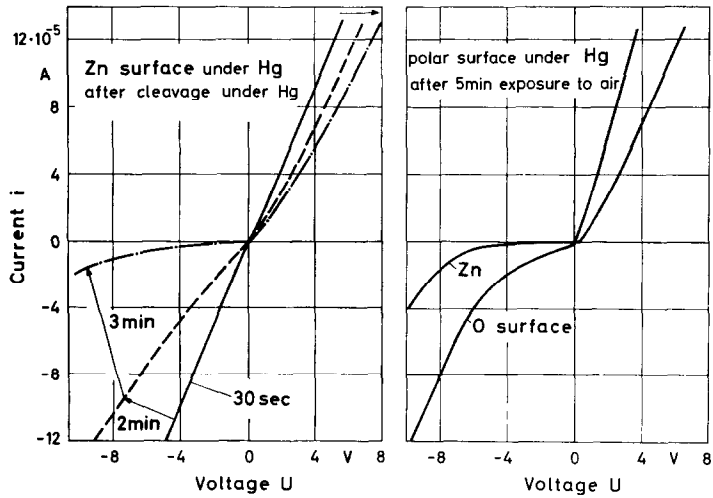

Fig. 11. Current voltage relations for the contact between mercury and the polar surfaces. After cleavage under mercury the O surface shows a corresponding curve, also initially without rectification. After Harreis[12]).

4.3. MEASUREMENTS OF REFLECTANCE

The reflectance of ZnO crystals exhibits changes up to several percent during changes of band bending by adsorption of gases[13]). Some results for

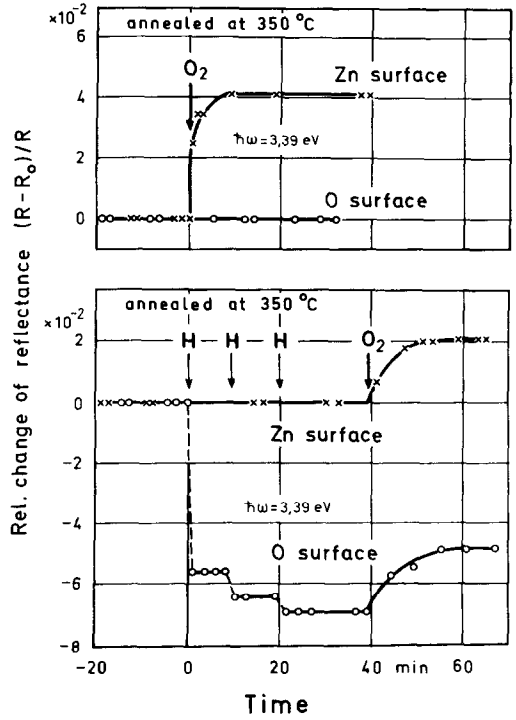

Fig. 12. Relative change of reflectance versus time after admission of oxygen (2 Torr) or atomic hydrogen and subsequently oxygen. After Hoffmann[13]).

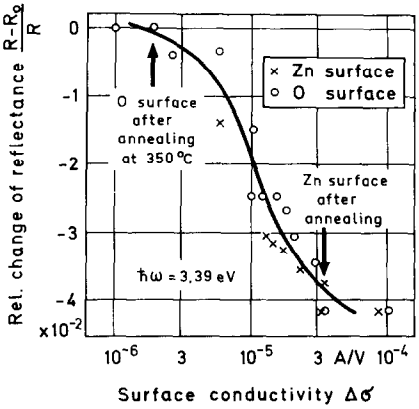

Fig. 13. Relative change of reflectance versus surface conductivity. One crystal, $\sigma_B = 5.7 \times 10^{-5}$ A/V cm. After Hoffmann[13]).

annealed polar surfaces are shown in fig. 12. There is a pronounced difference between the two types of surface. Before postulating a new polar optical effect, one should look at fig. 7 (after annealing). Then fig. 13 may be not so surprising: it shows that the difference for the two surfaces vanishes if the response is plotted versus surface conductivity. The limitation in quantum energy to a critical point of the band structure, the fundamental absorption edge, suggests an explanation corresponding to that of electroreflectance[14]). The high electric field in the space-charge layer changes the optical constants and reduces the reflectance. Therefore the reflectance decreases with growing bending of the bands (figs. 4 and 5), for depletion as well as for accumulation. The scale of surface conductivity in fig. 13 approximately resembles a scale of field strength at the surface.

5. Discussion

5.1. Atomic model

The sign of the *c* axis is opposite for the two polar surfaces. This is a reliable description, whereas atomic models are open to discussion. Gatos and Lavine[5] have proposed a surface bonding model for the {111}-surfaces of III–V compounds (zinc blende structure)[5]). It has also been applied to the wurtzite structure[6,2,15]). Fig. 14 shows the surface bonding model for ZnO.

The wurtzite structure exhibits a dipole moment due to termination of the crystal at the polar surfaces. If the bulk conductivity is sufficiently low, a change of polarization by variation of temperature (pyroeffect) or by elastic deformation (piezoeffect) is observable before the compensating charges are readjusted. Therefore a complete compensation by a shift of bound electrons does not take place.

From elastic and piezoelectric constants one infers a positive sign for the effective charge of the Zn atoms[3,16]). The amount is estimated to about one electronic charge. However, the determination of an effective ionic charge is usually based on changes of polarization. The "total" amount may be considerably lower than the "differential" one. Therefore the magnitude of the compensating charge remains unknown at present.

For cleavage perpendicular to the *c* axis two steps are considered: First the bonds are separated, leaving every surface Zn atom with $\frac{1}{2}$ electron in the free bond, and every surface O atom with $\frac{3}{2}$ electrons in the dangling bond. By addition of compensating charges these numbers may change. The compensating charges may form space-charge layers if they are not accommodated in surface states or dangling bonds.

Compensation during cleavage can be achieved not only by addition or

substraction of trapped or free carriers, but also by removal of one fourth of the uppermost layer of atoms on one surface and deposition on the other surface, i.e. splitting of the top double layers. The ratio is given by the relative distance of atomic layers along the c axis.

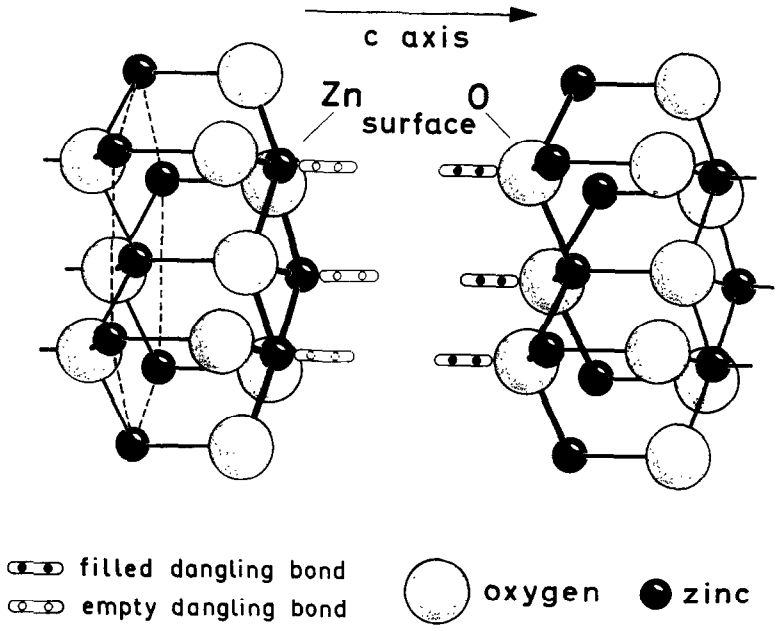

Fig. 14. Atomic model for the polar surfaces of ZnO (cf. fig. 6).

5.2. Clean surfaces

For the clean surfaces only an upper limit of surface conductivity and carrier density can be given. From the measured $\Delta\sigma < 4 \times 10^{-12}$ A/V, it follows that $\Delta N < 5 \times 10^{4}$ cm^{-2}, if the bulk mobility $\mu_B = 500$ cm^2/V sec is used. Therefore the compensating charge cannot be mobile. Immediately after cleavage under mercury, no depletion layer is detected on either surface (fig. 10). By comparison, a clean germanium surface shows a high p-type conductivity ($\Delta\sigma \approx 10^{-4}$ A/V), and a clean silicon surface is nearly intrinsic ($\Delta\sigma \approx 10^{-6}$ A/V for weak doping in the bulk).

Transient heat treatment results in a high conductivity on the Zn surface of 10^{-4} A/V, which corresponds to an electron density of about 10^{13} cm^{-2} at the limit of degeneracy ($\mu_S = 60$ cm^2/V sec). This accumulation layer may

contribute to the compensating charge. During annealing an irreversible structural transition can take place at the Zn surface and cause the high conductivity. According to the atomic model, the unfilled or partially filled orbitals of the Zn surface may induce a change in surface structure. Also a loss of oxygen during heating would result in an excess of zinc and the generation of donors, but the oxygen surface does not show an increase of conductivity by annealing. Furthermore, the possibility cannot be excluded that metallic impurities leave the Zn sublattice at the surface during annealing and become donors.

5.3. Action of hydrogen and oxygen

The density of hydrogen donors is also of the order of at least 10^{13} cm^{-2}. Atomic hydrogen increases the conductivity faster on the O surface, whereas oxygen decreases it faster on the Zn surface. In addition, without hydrogen pretreatment a depletion layer grows in oxygen faster on the Zn surface than on the O surface (fig. 11). These facts can be qualitatively interpreted in terms of filled and empty dangling bonds, similar to the discussion of etching behavior[5]). However the action of the gases includes two steps: adsorption with generation of donors or acceptors and change of electron concentration in the conduction band by these impurity centers. A separation would be possible with knowledge of sticking probabilities. The changes of reflectance confirm the results of conductance measurements. The dependence on surface conductivity shows that the conduction mechanism may not differ very much on both types of surfaces.

6. Conclusion

The discussion reveals that further studies of electrical and optical properties of polar surfaces are required before a more detailed model can be discussed. It will be of some interest to learn more about electronic states on polar surfaces. A crystal surface is not a separate entity, but is really the termination of the bulk. For the wurtzite structure one has to take into consideration not only the different types of atoms in the outer planes and the dipole layers at the surfaces, but also the internal polarization and the compensating charges. Furthermore a change of structure may take place within the top layers.

Acknowledgment

Discussions with Dr. H. Ibach and Dr. H. Lüth are gratefully acknowledged.

References

1) G. Heiland and H. Ibach, Solid State Commun. **4** (1966) 353.
2) A. N. Mariano and R. E. Hanneman J. Appl. Phys. **34** (1963) 384.
3) G. Heiland, P. Kunstmann and H. Pfister, Z. Physik **176** (1963) 485.
4) D. Coster, K. S. Knol and J. A. Prins, Z. Physik **63** (1930) 345.
5) H. C. Gatos and M. C. Lavine J. Electrochem. Soc. **107** (1960) 427.
6) E. P. Warekois, M. C. Lavine, A. N. Mariano and H. C. Gatos, J. Appl. Phys. **33** (1962) 690.
7) A. Klein, Z. Physik **188** (1965) 352.
8) G. Heiland, E. Mollwo and F. Stoeckmann, in: *Solid State Physics*. Eds. F. Seitz and D. Turnbull, Vol. 8 (Academic Press, New York, 1959) p. 191.
9) H. J. Krusemeyer, Phys. Rev. **114** (1959) 655.
10) G. Heiland, J. Phys. Chem. Solids **22** (1962) 227.
11) P. Kunstmann, Thesis, Aachen 1967.
12) H. Harreis, Aachen, private communication.
13) B. Hoffmann, Z. Physik **206** (1967) 293.
14) B. O. Seraphin and N. Bottka, Phys. Rev. **145** (1966) 628.
15) D. K. Smith, H. W. Newkirk and J. S. Kahn, J. Electrochem. Soc. **111** (1964) 78.
16) D. Berlincourt, H. Jaffe and L. R. Shiozawa, Phys. Rev. **129** (1963) 1009.
17) L. J. van der Pauw, Philips Res. Rept. **13** (1958) 1.
18) J. C. Monier and R. Kern, Bull. Soc. Franc. Mineral. Crist. **79** (1956) 495.